NASA-TM-111263

# AIAA 95-3945
# Equivalent Plate Modeling for Conceptual Design of Aircraft Wing Structures

Gary L. Giles
NASA Langley Research Center
Hampton, VA

**1st AIAA Aircraft Engineering, Technology and Operations Congress**
Los Angeles, CA
September 19-21, 1995

# EQUIVALENT PLATE MODELING FOR CONCEPTUAL DESIGN OF AIRCRAFT WING STRUCTURES

Gary L. Giles*

NASA Langley Research Center, Hampton, Virginia

## Abstract

This paper describes an analysis method that generates conceptual-level design data for aircraft wing structures. A key requirement is that this data must be produced in a timely manner so that it can be used effectively by multidisciplinary synthesis codes for performing systems studies. Such a capability is being developed by enhancing an equivalent plate structural analysis computer code to provide a more comprehensive, robust and user-friendly analysis tool.

The paper focuses on recent enhancements to the Equivalent Laminated Plate Solution (ELAPS) analysis code that significantly expands the modeling capability and improves the accuracy of results. Modeling additions include use of out-of-plane plate segments for representing winglets and advanced wing concepts such as C-wings along with a new capability for modeling the internal rib and spar structure. The accuracy of calculated results is improved by including transverse shear effects in the formulation and by using multiple sets of assumed displacement functions in the analysis.

Typical results are presented to demonstrate these new features. Example configurations include a C-wing transport aircraft, a representative fighter wing and a blended-wing-body transport. These applications are intended to demonstrate and quantify the benefits of using equivalent plate modeling of wing structures during conceptual design.

## Introduction

The design process for aerospace vehicles progresses through conceptual, preliminary and detailed design phases in which the sophistication of the analysis methods and the quality of the design data increases. During conceptual design, many alternative configurations are evaluated in multidisciplinary design trades to determine the values of system-level variables (e.g., type and number of engines), the size (gross weight) and shape (external geometry parameters) of a candidate configuration which will best meet a specified measure of overall vehicle performance. A representative configuration sizing code for use in conceptual design is the Flight Optimization System (FLOPS)[1] which operates on such system-level design variables.

Typically in such codes, use is made of relatively simple, experience-based equations or elementary analytical models to relate these system design variables to the important vehicle characteristics from each engineering discipline such as aerodynamic lift and drag and structural weight. This implicit, experience-based design data should not be used beyond its limits of validity. However, characteristics of advanced aircraft concepts often exceed these limits and user judgment is required to adjust and extrapolate the available data in order to perform system studies. Hence, there is a continuing need to improve the quality of conceptual design data through use of explicit, physics-based analysis methods early in the design process

Airframe weight is the key structural parameter used in aircraft system studies. In conceptual and early preliminary design, empirical weight equations are often used to calculate this data. These equations are principally functions of the vehicle class and external geometry and require very little information about the internal structural details. In later design phases, the locations and sizes of an assemblage of structural members making up the airframe are determined. The airframe should be lightweight but also have sufficient strength and stiffness necessary to satisfy all the requirements throughout its flight envelope. General purpose finite element structural analysis codes are available to model and analyze the static and dynamic response of airframes in great detail. However, such analyses usually require considerable calendar time to generate the finite element model and repetitive analyses can be computationally expensive.

This paper will describe an analysis method that is intended to generate conceptual-level design data for aircraft wing structures. It is a design-oriented structural analysis method[2] that is intended to bridge the gap between weight equations and detailed finite element analyses. This capability is being developed by enhancing the Equivalent Laminated Plate Solution (ELAPS) computer code[3-5] to provide a more comprehensive, robust and user-friendly analysis tool. A key requirement is that the design data must be produced in a timely manner so that it can be used effectively by multidisciplinary synthesis codes for performing systems studies.

The present paper will focus on recent enhancements to the ELAPS code that significantly expand the



*Senior Research Engineer, Systems Analysis Branch, Aeronautics Systems Analysis Division, Associate Fellow AIAA.

modeling capability and improves the accuracy of results. Modeling additions include use of out-of-plane plate segments for representing winglets and advanced wing concepts such as C-wings along with a new capability for modeling the internal rib and spar structure. The accuracy of calculated results is improved by including transverse shear effects in the formulation and by using multiple sets of assumed displacement functions in the analysis.

Typical results are presented to demonstrate these new features. Example configurations include a C-wing transport aircraft, a representative fighter wing and a blended-wing-body transport. These applications are intended to demonstrate and quantify the benefits of using equivalent plate modeling of wing structures during conceptual design.

## Equivalent Plate Modeling

A wing box structure is represented as an equivalent plate in this formulation. Planform geometry of this equivalent plate is defined by multiple trapezoidal segments as illustrated by the two-segment box in Fig. 1. Each plate segment has upper and lower cover skins which may contain multiple layers of composite material. The cross-sectional view of a typical segment illustrates the generality to define out-of-plane shapes such as the twist and camber characteristics of an aircraft wing. The cross-sectional dimensions of wing depth, camber definition and cover skin thicknesses are defined by polynomials which vary over the planform of each segment. For static analysis, loading is applied to the wing box as concentrated forces or distributed loads. Mass properties for dynamic analysis are defined by concentrated or distributed quantities.

The specification of model characteristics as continuous distributions in polynomial form on only a few members requires only a small fraction of the volume of input data for a corresponding finite element structural model where geometry and stiffness properties are specified at discrete locations. The resulting reduction in model preparation time is important during early design phases when many candidate configurations are being assessed. Also, the geometric locations of the mass quantities and the applied loadings can be independently defined, i.e., they are not referenced to a set of joint locations as in a finite element model. The ease of relocating these quantities without disrupting other aspects of the model is important during early design when such changes often occur. Finally, the polynomial description of model characteristics lends itself to use with optimization algorithms since the polynomial coefficients can be used directly as design variables. Therefore, the analytical formulation in ELAPS requires minimal time for model preparation and modification.

The analysis procedure, outlined in Fig. 2, is based on the Ritz method in which the deflection of the structure is described by assumed polynomial displacement functions. In order to achieve a high level of computational efficiency, the displacement functions $U$, $V$ and $W$ are defined by combinations of terms from a power series in the chordwise coordinate $x$ and a power series in the spanwise coordinate $y$. as indicated in the figure. These $x$ and $y$ coordinates are non-dimensionalized by dividing by a reference length (usually the wing semispan) so that the coefficients all have the same units of length. Substituting these functions into the expression for total energy and differentiating to minimize the energy produces a set of linear, simultaneous equations which can solved for the desired set of unknown polynomial coefficients. These coefficients are used to calculate deflections, strains and stresses over the planform of the plate segments. Typically, the number of terms in the polynomial displacement functions is relatively small (around a hundred) and results in efficient computation. The number of terms is selected by the user. In this manner, the user is given the capability to trade accuracy for speed. However, there are upper limits on the degree of the polynomials that can be specified for the displacement functions. This limit results from using power series terms which are non-orthogonal. High-degree terms produce nearly linearly dependent equations and cause the set of governing equations to become ill-conditioned. Typical, practical upper limits on the power series terms are fourth degree in $x$ and seventh degree in $y$.

## Modeling Enhancements

A design oriented structural analysis code needs to be capable of modeling a wide variety of advanced concepts and needs to include all the primary structural members. Recent enhancements to ELAPS include modeling of wings composed of segments that are not all in the same plane and adding capability to include rib and spar shear webs in the structural model. In order to calculate the deformation and stresses of the rib and spar webs, transverse shear considerations must be included in the analytical formulation. These additions are discussed in this section. The details of the approach used to include transverse shear effects are described in Appendix A.

### Out-of-plane modeling

The addition of out-of-plane modeling provides the capability to perform structural analysis of unconventional, advanced wing concepts[6] such as the C-wing[7] shown in Fig. 3. The various portions of such a wing are modeled as shown in Fig. 4a by using equivalent plate segments whose positions are defined by newly added local analysis reference planes. These reference planes are connected by sets of very stiff springs with the goal of providing approximate displacement continuity at the juncture of adjacent plate segments. This approach provides a good approximation to having equal displacements in each plate, if sufficiently large values of spring stiffnesses are used. The motions of the upper and lower wing cover skins are governed by motions of the reference planes via rigid, straight lines that remain normal to these deformed surfaces as illustrated in Fig. 4b for a single point that is representative of all points over the surface. Since only the reference planes are connected in this formulation, it eliminates the time-consuming complexity of matching

all the joint locations along boundaries of adjacent components (at both the upper and lower surfaces) of the actual wing structure that is required for conventional finite element modeling.

Each of the local analysis reference planes are defined with respect to the global reference frame. In the current implementation, the inboard and outboard edges of the local reference frames are defined to be parallel to the global $x$-axis that is oriented in the chordwise direction of the wing, usually along the centerline of the vehicle. Therefore, the position of each reference plane is defined by an angular rotation about the $x$-axis relative to the $x$-$y$ plane. These reference planes provide the capability to model wings with dihedral and/or tip fins as well as more complex geometries such as C-wings. The sets of stiff springs are not restricted to lie in the analysis reference plane. Hence, they can be defined near the mid-camber location of adjacent segments of the wing structural box or located along the hinge line of control surfaces or at locations of boundary condition constraints.

The coordinate systems for the stiff springs are defined with respect to the global coordinate system in order to resolve the different spatial orientations of the plate segments. The strain energy of the springs must be expressed in terms of the displacement function coefficients so that contributions to the overall stiffness matrix can be evaluated. This relationship is expressed in terms of a transformation matrix $[T_4]$ as

$$\{\delta_1\ \delta_2\ \delta_3\ \theta_1\ \theta_2\ \theta_3\}^T = [T_4]\ \{C_u\ C_v\ C_w\ C_{\phi x}\ C_{\phi y}\}^T \quad (1)$$

The terms $\delta_1$, $\delta_2$, $\delta_3$ define spring translations and $\theta_1$, $\theta_2$, $\theta_3$ define spring rotations. The terms $C_u$, $C_v$, $C_w$ are coefficients for displacement functions in the x,y,z directions respectively and $C_{\phi x}$ and $C_{\phi y}$ are coefficients for transverse shear deformation to be discussed in the next section.

The overall transformation matrix, $[T_4]$, is formed as the product of three individual transformation matrices as

$$[T_4] = [T_1]\ [T_2]\ [T_3] \quad (2)$$

Taken individually, the elements of $[T_1]$, $[T_2]$, $[T_3]$ are straightforward to evaluate. Therefore, for brevity only a brief narrative description of each matrix is given to avoid a lengthy and detailed geometric definition and description of the various coordinate systems that are involved.

$[T_1]$ is used to transform deformations from the global coordinate system to the same deformations in a spring coordinate system.

$[T_2]$ is used to transform deformations from the coordinate system of a local analysis reference plane to the same deformations in the global coordinate system.

$[T_3]$ relates the deformations of a local analysis reference plane that correspond to deflections that are evaluated at the locations of the springs to the coefficients of the polynomial displacement functions. The reference plane deformations are calculated by multiplying the polynomial coefficients by $[T_3]$.

Elements of the $[T_1]$ and $[T_2]$ matrices are composed of direction cosines of a spring coordinate system and a coordinate system of a local analysis reference plane since both of these coordinate systems are defined with respect to the global coordinate system. Calculation of elements of $[T_3]$ involves evaluation of the expressions for translations and rotations given in Eqs. (A.1)-(A.5), where $z$ is the perpendicular distance from the analysis reference plane to a spring of interest and $x$ and $y$ are its coordinates in the analysis reference plane.

The stiffness matrix of a spring, $[K_s]$, is composed of six diagonal elements corresponding to values for spring constants in the three translational and three rotational directions. The contribution of an individual spring, $[K_s]$, to the overall or system stiffness matrix, $[K_{sys}]$ is given by

$$[K_{sys}] = [T_4]_a^T [K_s] [T_4]_a - [T_4]_a^T [K_s] [T_4]_b + [T_4]_b^T [K_s] [T_4]_b \quad (3)$$

where the subscripts $a$ and $b$ refer to two different local analysis reference planes that are connected by the spring.

For static analysis, rigid-body motion of the equivalent plate must be constrained. These constraints are often referred to as boundary conditions. The stiff springs can be used to constrain the translations and/or rotations at selected locations. For this use, the displacement system denoted by the subscript $b$ is taken to be zero, thus only the first triple product in Eq. (3) is evaluated. Although displacements cannot be specified to be exactly zero at a selected location, use of sufficiently stiff springs will provide a good approximation to the desired condition. An additional method of specifying boundary conditions is provided for use in vibration analysis. A eigenvalue shift parameter has been included that allows a vibration analysis to be performed on a model with unconstrained (rigid-body) motions.

**Modeling of ribs and spars**

The capability to model ribs and spars has been added through the use of caps located at the upper and lower cover skins and corresponding shear webs through the depth of the wing. Sets of ribs or sets of spars are defined with respect to the corresponding plate segment planform definitions. Examples of sets of ribs and spars are illustrated by the planform layouts shown in Fig. 5. A minimal number of input quantities are used to define the geometric layout of these ribs and spars.

A set of ribs is defined by specifying the total number of ribs that are to be evenly spaced between the inboard and outboard edges of a plate segment. This number includes the ribs along the inboard and outboard edges in addition to the intermediate ribs. The rib definition is very straightforward since all ribs are parallel and are located in the chordwise direction.

Three options are available for defining sets of spars. In the first option the spars are all parallel to the trailing edge of the plate segment and the specified number of spars are spaced equidistant along the inboard edge as shown in Figs. 5a and 5b. The second option is similar to the first option except that the spars are all parallel to the leading edge of the segment as shown in Fig. 5c. In

the third option, the spars are "fanned out" between the leading and trailing edges with the ends evenly spaced on both the inboard and outboard edges as shown in Fig. 5d.

The cross sectional areas of the caps and the thicknesses of the shear webs are specified by polynomials that are defined over the planform of a plate segment. The values for areas and thicknesses at any location on an individual rib or spar are obtained by evaluating the appropriate polynomial at the location of interest. Therefore, the member sizes within a set can change from rib to rib or spar to spar and also vary along their lengths. This polynomial description of rib and spar member properties is useful in design studies in that it links all member sizes using a small number of polynomial coefficients that can be used as design variables. Also, the cross-sectional dimensions can be evaluated along the length of each individual member during structural weight calculations.

In the analysis formulation, the discrete stiffness properties of these members are "smeared" to form an approximate, continuous representation over the planform of a segment. This approach permits tables of integrals that are calculated over the segment planforms for generating the stiffness matrices for the cover skins to also be used for the ribs and spars. Hence, the smeared representation provides a significant reduction in computational time compared to forming the required integrals for each individual rib and spar.

Terms for the shear web contribution to the overall stiffness matrix are obtained from the equations that are produced by differentiating the energy expression of the webs with respect to the coefficients of polynomials that describe the transverse shear. The energy of a set of smeared webs is given by

$$E = (G/2) \int_{area} \int_z [\,(h)\,(t_{smeared})\,(\gamma_{lz})^2\,]\,dz dA \qquad (4)$$

where $G$ is the shear modulus of the material,
$h$ is the depth of the wing,
$t_{smeared}$ is the equivalent thickness of the web,
$\gamma_{lz}$ is the transverse shear strain in the web.

Integration is performed between the upper and lower skin surfaces and over the planform of a plate segment

For ribs:

$t_{smeared} = t_{discrete}$ * (no. of ribs) / (span of segment)
and $\gamma_{lz} = \phi_x$

For spars:

$t_{smeared} = t_{discrete}$ * (no. of spars) / (local chord * $dy/dl$)
and $\gamma_{lz} = \phi_x * dx/dl + \phi_y * dy/dl$

where $t_{discrete}$ is the thickness of a discrete web,
$\phi_x$ and $\phi_y$ are transverse shear displacement functions described in the next section,
$l$ is along the length of a web.

These calculations for shear webs involve consideration of transverse shear effects that is discussed in the next section.

**Transverse shear consideration**

During early studies of a High Speed Civil Transport (HSCT) wing at the Boeing Company[8], it was concluded that for some applications it was important to include the effects of transverse shear in the equivalent plate formulation in order to improve the accuracy of the analysis results. The option to include transverse shear effects has been added to ELAPS in conjunction with the modeling of rib and spar webs.

The analysis formulation of Ref. 4 is developed in terms of expressions for the bending and stretching of a reference plane. This formulation has three sets of assumed displacement functions; $U$ and $V$ are in-plane and $W$ is normal to the reference plane. The motions of the upper and lower wing cover skins are governed by motions of the reference plane via rigid, straight lines that remain normal to the deformed reference plane. In order to include transverse shear in the formulation additional degrees of freedom are added which allow the straight lines to be oriented at angles other than 90 degrees (not normal) to the reference surface. These degrees of freedom are formulated as additional rotations in the $x$ and $y$ directions with respect to the reference surface normal and are defined using two new sets of assumed displacement functions $\phi_x$ and $\phi_y$. The details of the transverse shear formulation used herein are presented in Appendix A. This formulation results in transverse shear strain and stresses that are constant throughout the depth of the wing but vary over the planform. Thus, the shear strain is constant through the depth of a rib or spar web but can vary along its length.

In the present analysis, the assumed displacement functions are formulated in a manner that allows the shear deformation terms to be either included or neglected (set to zero) through specification of a few user input parameters. Therefore, the importance of transverse shear effects for a particular application can be assessed quickly and may be neglected if the effects are small in order to minimize computational time. This ability to neglect transverse shear during early design cycles and to include it in later cycles provides a hierarchical analysis procedure with the option to trade accuracy for computational speed; a desirable feature for use during conceptual design. In contrast, the displacement formulation for conventional first order shear deformation plate theory, as used in Ref. 9, does not allow the shear deformation terms to be simply set to zero. A comparison of the two formulations is given in Appendix A.

**Mass modeling enhancements**

During conceptual design studies, one of the key considerations is the modeling of overall vehicle weight or mass. Enhancements that have been made to ELAPS which facilitate modeling of masses that are important for wing design are discussed in this section. Major considerations include items such as the main structural box, the leading and trailing edges including any control surfaces, fuel carried in the wing, and wing mounted engines and pylons. The mass of the idealized structural box is calculated as the product of the density and volume of material in the equivalent plate structural

model. Currently, this idealized structural mass is multiplied by a correlation factor to approximate a value for actual structural mass. This correlation factor is usually obtained by performing an equivalent plate analysis of an existing, baseline vehicle with known measured masses.

User input of concentrated masses was available in earlier versions of ELAPS for representing a variety of sources of non-structural mass. The capability to readily model mass that is distributed over the wing planform has been added to the present version. This mass can be uniformly distributed over the planform area and/or throughout the internal volume between the upper and lower surfaces of each plate segment. The user is given the option to input either total or unit masses corresponding to the area or volume of each plate segment. This capability allows leading and trailing edge structural mass to be easily distributed over the appropriate areas of the wing planform and fuel mass to be readily distributed within designated volumetric regions of the wing.

This user defined mass model is used to calculate a variety of mass related quantities. The integral tables that were formed to generate the stiffness matrix of the structure are used in these calculations. Total mass of all structural members and all non-structural items that are contained in the model is calculated along with the first and second moments of inertia with respect to the global axes. The center of gravity location is then calculated by dividing the first moments of inertia by the total mass. This total mass and inertia data is available for use in stability and control calculations during early conceptual design.

Inertia relief loads are calculated based on input of a value of maneuver load factor. These inertia relief loads are combined with the aerodynamic loads to give loads that are used for structural design. In addition, a mass matrix is generated for the entire model for use in vibration analysis to calculate natural modes and frequencies.

### Solid Modeling for Aeroelastic Calculations

The integral tables for the planform of the equivalent plate segments were extended to include terms for integration through the entire depth of the wing in addition to the previous terms for integration through the cover skins. These new tables can be used to form the stiffness matrix for wings that have solid material between the upper and lower surfaces. Wind tunnel models are often constructed in this manner in an attempt to minimize model deflections to a level that resulting effects on measured aerodynamic data can be neglected.

The ELAPS solid modeling capability was used to analyze a solid wind tunnel model of a high aspect ratio transport wing that was recently tested in the National Transonic Facility.[10] This equivalent plate model was coupled with an unstructured-grid Euler flow solver with an interacting boundary layer method to perform a series of aeroelastic analyses as described in Ref. 11. Including the aeroelastic effects in the calculated wing pressures improved the comparison with measured wind tunnel data. Up to 19,917 surface nodes were used in the unstructured aerodynamic grid. The effort required to combine the loads and the deflections from the unstructured aerodynamic analysis and the equivalent plate model was minimal because of the continuous definition of the wing deflection in ELAPS. Also, when the number and location of the surface nodes in the aerodynamic grid was changed, the corresponding forces were calculated in a consistent manner without any modifications to the codes.

The relatively small size of the ELAPS code offers the practicality of embedding it directly into the iterative procedure of any CFD code so that such a combined code would converge to an aerodynamic solution on a deformed shape with a minimal increase in computational time over that required for the analysis of a rigid shape. In addition to the application outlined herein, equivalent plate models can be used effectively very early in the design process to assess the importance of aeroelastic effects on advanced concepts before detailed finite element models are available.

### Levels of Analysis

Input parameters are available in ELAPS to provide user control of the level of detail to be included during an analysis. In this manner, the user is given the capability to trade accuracy for computational speed. This capability is beneficial during conceptual design since initial design cycles can be performed at a low level of detail that can be easily increased during later cycles. This approach can be particularly advantageous when ELAPS is used in a structural optimization procedure that requires a large number of analyses during each iterative design cycle. The level of analysis in ELAPS can be controlled without changing the geometric definition of the model. Rather, the total number of unknown quantities in the resulting set of governing equations is readily changed by specifying a few input parameters. Three methods are available for selecting the level of detail to be included in an analysis.

Method 1: Select which deformations ($U$, $V$, $W$, $\phi_x$, $\phi_y$) are to be included in a set of displacement functions.

Method 2: Specify the number of terms used to define each deformation quantity.

Method 3: Specify multiple sets of displacement functions to be used in an analysis.

With Method 1, the most elementary level of analysis is selected by using only the out-of-plane bending deformation, $W$. This modeling is valid for pure bending (no transverse shearing) of symmetric equivalent plate models of thin wing structures representative of fighter aircraft and for modeling of aerodynamic control surfaces. The next level of analysis includes the inplane deformations $U$ and $V$ in addition to $W$. This level can be used to represent unsymmetric plate structures that result from wing camber and twist and/or cover skins that are not the same thicknesses on the upper and lower surfaces. Finally, transverse effects can be included with

the addition of $\phi_x$ and $\phi_y$ to the set of displacement functions. Transverse shear deformation can be significant for thick wing configurations and in designs with low shear stiffness resulting from a small number of ribs and spars and/or from small web thicknesses. The effects of neglecting some of these deformations can be quickly assessed for a given configuration to establish the appropriate level of analysis needed for a particular aspect of conceptual design.

With Method 2, the degree of the polynomials that are summed to form each displacement function are specified. Combinations of terms from a power series in the chordwise direction $x$ and a power series in the spanwise direction $y$ were used in the previous versions of ELAPS. There are upper limits on the degree of the terms in the power series. These upper limits are problem dependent but typical exponents are 6 or 7. Increasing the degree produces an ill-conditioned set of governing equations and the upper limit is reached when the solution subroutine terminates with a message to indicate excessive numerical error. The previous versions of ELAPS used an equation solver based on Cholesky decomposition. In the present version, an option is provided to use a solver that incorporates Gaussian elimination with a full pivoting strategy. It was found that when the Gauss solver is used the exponents could be increased by 1 or 2 over the upper limit used by the Cholesky solver.

Two approaches were studied in an attempt to overcome the ill-conditioning problem. In the first approach, direct generation of the governing equations using orthogonal polynomials was evaluated. This approach was found to require significantly more computational time than the very efficient power series implementation. The second approach was investigated in which the set of governing equations were generated using powers series and then transformed to a set of equations with basis functions from a family of orthogonal polynomials. This approach was implemented by appropriate pre- and/or post-multiplying both the stiffness and mass matrices and load vectors by a transformation matrix that related the orthogonal polynomials to the polynomials composed of power series. Options to select Legendre, Chebyshev or Hermite orthogonal polynomials were implemented and tested. This approach proved to be unsuccessful in that attempts to use exponents for terms in the orthogonal polynomials that were greater than the upper limit used for power series either caused the solution subroutines to terminate or the analysis results to diverge. Considerable effort was devoted to the second approach because of the potential simplicity that would be gained through use of a single set of very high-order, orthogonal displacement functions to represent the behavior of all plate segments in a wing structure.

Method 3 was tested by using multiple sets of displacement functions with each set governing the behavior of a selected grouping (subset) of the plate segments in the model. These sets of displacement functions were connected using the stiff springs discussed in the out-of-plane modeling section. Method 3 was found to give increased accuracy while not producing excessively large matrices and provides a recommended alternative to the implementation of Method 2.

## Applications and Results

Results are presented in this section from selected example applications that demonstrate the new equivalent plate modeling features of the ELAPS code. These examples are intended to illustrate the variety of structural analyses that can be performed and the kinds of calculated data and the levels of accuracy that can be produced for use in conceptual design studies.

### C-wing Example

In the first example, the wing structure for a C-wing transport configuration shown in Fig. 3 is analyzed to demonstrate the use of the new out-of-plane modeling capability. A schematic of a semispan equivalent plate of this wing is shown in Fig. 6. Four plate segments, numbered 1-4, are used to model the C-wing structure. Segments 1 and 2 represent the main wing box and segments 3 and 4 represent the vertical and horizontal fin portions of the C-wing respectively. Segment 3 has a constant chord and has the same sweep as the leading edge of the main box. One set of stiff springs are used to provide cantilever boundary conditions at the centerline of the wing and two other sets are used to connect segment 2 to segment 3 and to connect segment 3 to segment 4. A conventional planar wing that has an extended tip added to the main box (outlined in dashed lines) is also shown superimposed to the same figure. The planar wing is composed of segments 1, 2 and 5. Segment 5 of the planar wing is the same size and shape as segment 4 of the C-wing. The depths of the segments, $h$, have a linear spanwise variation and have a constant value in the chordwise direction

Analyses are performed to compare results for the C-wing and the planar wing under comparable applied loads. A uniform pressure load of 1.0 psi acting upward is applied to the planar wing. The C-wing is analyzed for two separate loading cases. In both cases, uniform upward pressure is applied on segments 1 and 2 and no load is applied to segment 3. However, the pressure load on segment 4 acts upward in the first load case and acts downward in the second load case. A pressure load of 1.0 psi is used for the first load case which gives the same total lift as for the planar wing. The pressure load is increased to 1.306 psi in the second load case to provide to same total lift because of the downward pressure on the horizontal fin.

The vertical deflections of the leading and trailing edges along the semispan of the main box (segments 1 and 2) are shown in Fig. 7. The planar wing has the largest tip deflection. The C-wing with an upward loaded horizontal fin has less vertical tip deflection but has more tip twist as indicated by the larger difference in vertical deflections of the leading and trailing edges. The C-wing with a downward loaded fin has significantly less deflection and the tip is twisted to have a positive angle-of-attack.

Spanwise stresses in the upper and lower cover skins at the trailing edge of the main box are shown in Fig. 8.

The planar wing has compressive stresses in the upper cover skin and tensile stresses in the lower cover skin. These stresses increase from tip to root which is expected for a constant cover skin thicknesses used for this illustrative example. The C-wing has some unusual stress distributions at the tip of the main wing box. These unusual distributions are caused by the moments that are produced by loading on the horizontal fin. In the case of the upward loading, the cover skin stresses actually change sign at approximately 85 percent semispan. In the case of downward loading, the cover stress is approximately zero in the 75 percent semispan region but remains in compression in the upper skin and tension in the lower skin of the outboard region. Additional studies are required to determine if control of the loading on the horizontal fin can be used to reduce the structural weight of the main wing box as a result of the lower stresses. This potential structural improvement must be traded against the effects on aerodynamic drag that would occur. The ELAPS analysis code can provide the structural data needed to investigate such questions during early conceptual design.

In addition, the first ten vibration frequencies for the C-wing and the planar wing are compared in Fig. 9. The frequencies of the C-wing are significantly lower that for the planar wing indicating that aeroelastic phenomenon such as flutter should be analyzed in subsequent studies.

**Clipped-delta Example**

A representative example of a fighter wing structure that was studied in Ref. 4 is used herein to assess the accuracy of the newly implemented smeared web modeling capability and the new transverse shear formulation in ELAPS. The planforms of the equivalent plate model and a finite element model used for comparison are shown in Fig. 10. The planforms are composed of a clipped-delta outer segment with a 45 degree leading edge sweep and an inner segment that is used to represent a carry-through structure.

In this study, rib and spar shear webs are incorporated in the equivalent plate model. These rib and spar webs are located vertically through the depth of the wing box along the lines that define the mesh shown in the finite element model. A smeared representation of these webs is used in the equivalent plate formulation while discrete shear elements are used in the finite element model.

Static analyses were performed with three different thicknesses in all rib and spar webs; $t_{web}$ = 0.01, 0.10 and 5.0 inches. The web thickness of 5.0 is unrealistically large but is used in the finite element model to approximate the condition of infinite shear stiffness (no shear flexibility). For this case ELAPS was run with the transverse shear displacement functions set equal to zero. A uniform pressure load of 1.0 psi is applied to the outer segment of the wing. Values of vertical displacement at the trailing edge of the wing tip as indicated in Fig. 10 are compared. These results are shown in Fig. 11. The tip deflection increases only slightly when the web thickness is reduced from 5.0 to 0.1. The finite element and equivalent plate results are in close agreement for $t_{web}$ = 5.0 and 0.1. Transverse shear effects are more pronounced when the web thickness is reduced to 0.01. In this case ELAPS gives a 7 percent larger deflection than the finite element analysis.

The shear stress distributions are compared along the semispan of the selected spar that is indicated in Fig. 10. These results are shown in Fig. 12 for a web thickness of 0.1. The shear stresses for ELAPS are greater than for the finite element analysis. Also, a discontinuity in shear stress occurs between the inner and outer plate segments. The stiff springs used to connect the two segments enforce approximate continuity of displacements but the strains and stresses may be discontinuous as shown in Fig. 12. The stresses from the two analyses exhibit the same trends and the equivalent plate results are shown to be of sufficient accuracy for use in conceptual design studies.

**Blended-Wing-Body Example**

The use of ELAPS for structural sizing is illustrated by this example. Also, use is made of the new capabilities for mass modeling. The aircraft configuration used in this study is an advanced blended-wing-body[12] large subsonic transport that offers potential performance benefits. A schematic of a representative configuration is shown in Fig. 13. The inboard region of this vehicle has sufficient depth to accommodate a double deck passenger cabin with a theater-like seating arrangement. Candidate structural concepts for carrying the cabin pressure loads include (a) a self-contained pressure vessel that is suspended inside of the wing box structure and (b) use of sandwich skins with sufficient depth to carry the local bending moments produced by the cabin pressure. The present study is representative of concept (a) in that cover skins of the main box structure are sized to carry only the aerodynamic loads.

A planform view of a semispan equivalent plate model of this vehicle is shown in Fig. 14. A total of 18 plate segments are contained in the model. Segments 1-6 represent the main structural box; segments 7-12 are used to represent the leading edge; and segments 13-18 are used to represents the trailing edge region of the wing. The spanwise stiffness of the material in the leading and trailing edge is reduced so that no spanwise wing bending loads are carried by these regions. However, any loads that are applied to these regions are properly transmitted fore and aft to the main box structure. The depth and camber of each plate segment is specified as products of cubic polynomials in the spanwise and chordwise directions. A single set of displacement functions is used to govern the displacements in all 18 plate segments.

Representative non-structural masses that are included in the model are also indicated in Fig. 14. The capability to distribute mass uniformly over the planform area of a segment is used to represent the mass of passengers in segments 1 and 2. The capability to distribute mass within the volume between the upper and lower surfaces of a segment is used to represent the fuel mass in segments 3 and 4. The contributions to the overall mass matrix of the model are calculated in ELAPS by integrating the products of the masses in

these areas and volumes with the displacement functions over the planforms of these segments. Total masses associated with each segment is all the user input that is required. Concentrated masses are used to represent localized components such as landing gear and engines as shown in Fig. 14. A single mass is used for each landing gear and the engine weight is distributed among five masses along the length of the engine. The $x$, $y$, $z$ coordinates and magnitude of each mass is all the required user input. This straightforward, simple method of defining a mass model is very useful during conceptual design. The time-consuming operation of distributing these various masses to grid points in a finite element model is avoided in the equivalent plate approach. The structural and non-structural masses are used to calculate the first and second moments of inertia of the vehicle along with the total mass and center of gravity location. Inertia relief loads are also calculated corresponding to maneuver load factors that can be input by the user. A 2.5g symmetric pull-up maneuver is used as a representative design condition in this study. An elliptical spanwise distribution of aerodynamic pressure is assumed. This pressure is distributed over all 18 planform segments.

The thickness distribution of the cover skins in the main wing box is sized using a manual iterative procedure. In each iteration cycle, Von Mises stresses in the cover skins are calculated using ELAPS. Then, the skin thickness values over the planform are increased or decreased by the ratio of the calculated Von Mises stress to the allowable stress of the material. The thicknesses of the upper and lower skins are assumed to be the same. This so-called fully-stressed design procedure converged in three cycles. The resulting skin thickness distribution along the semispan of the wing is shown in Fig. 15. The large thickness that occurs in the vicinity of the trailing edge break, y/semispan = 0.45, could be reduced by increasing the wing chord and corresponding wing depth at that location. Such a design change to improve the structure would have to be traded against the effect on aerodynamic performance that would occur. This example indicates the necessity to be able to use ELAPS in a multidisciplinary design system to perform overall system level design trade studies. The recent enhancements to ELAPS have been demonstrated to provide an effective design tool for such purposes in that the major considerations in the design of aircraft wing structures can be analyzed in a timely manner.

## Concluding Remarks

Recent developments in equivalent plate modeling are described. These modeling methods are for use in design and analysis of aircraft wing structures during conceptual design studies before the external shape of the vehicle is fixed. The capability to define out-of-plane plate segments has been added for representing winglets and advanced concepts such as C-wing configurations. A more complete representation of a wing structure is provided by the addition of rib and spar shear webs. The analysis formulation is expanded to include the effects of transverse shear deformations. This formulation provides shear stresses in the rib and spar webs and also improves the accuracy of the wing deflections and cover skin stresses over previous versions of ELAPS that neglected transverse shear effects. These enhancements are implemented such that the user can easily control the level of detail to be included during an analysis. This control is beneficial during conceptual design since accuracy of results can be traded for computational speed in order to maximize the effectiveness of overall structural design procedures. An additional capability allows leading and trailing edge structural mass to be easily distributed over appropriate areas of the wing planform and fuel mass to be readily distributed throughout designated regions of a wing. Overall mass and inertia properties are calculated along with inertia relief loads. These additions provide a versatile equivalent plate analysis tool that can model the physical behavior of the major components that must be considered in wing design and can effectively produce structural-related data for use in performing systems studies during conceptual design.

Typical results are presented to demonstrate these new features. A C-wing transport aircraft is used to illustrate out-of-plane modeling capability. A representative fighter wing is use to illustrate the modeling of rib and spar webs along with the use of the transverse shear formulation. A blended-wing-body transport is used to illustrate the use of new mass modeling capabilities and to demonstrate a manual structural sizing procedure. These applications demonstrate and quantify the benefits of using equivalent plate modeling of wing structures during conceptual design.

## Appendix A
## Transverse Shear Formulation

The analysis formulation of Ref. 4 is developed in terms of expressions for the bending and stretching of a reference plane. The motions of the upper and lower wing cover skins are governed by motions of the reference plane via rigid, straight lines that remain normal to the deformed reference plane. In order to include transverse shear in the formulation additional degrees of freedom are added which allow the straight lines to be oriented at angles other than 90 degrees with the reference surface. These degrees of freedom are defined as additional rotations in the $x$ and $y$ directions with respect to the reference surface normal.

Displacements and rotations throughout the wing are approximated by

$$U = U_O - z\,W_{O,x} + z\,\phi_x \qquad \text{(A.1)}$$

$$V = V_O - z\,W_{O,y} + z\,\phi_y \qquad \text{(A.2)}$$

$$W = W_O \qquad \text{(A.3)}$$

$$\theta_U = W_{O,y} - \phi_y \qquad \text{(A.4)}$$

$$\theta_V = W_{O,x} - \phi_x \qquad \text{(A.5)}$$

where $\phi x$ and $\phi y$ are the two new rotational displacement fields. In the Ritz analysis procedure, these displacement fields are specified as products of terms from a power series in the $x$ direction with terms from a power series in the $y$ direction as is done for the $U$, $V$, and $W$ components of the deformation .

Corresponding strains in the skins in the $x$ and $y$ directions are given by

$$\varepsilon_x = U_{o,x} - zW_{o,xx} + z\phi_{x,x} \qquad (A.6)$$

$$\varepsilon_y = V_{o,y} - zW_{o,yy} + z\phi_{y,y} \qquad (A.7)$$

$$\varepsilon_{xy} = U_{o,y} + V_{o,x} - 2zW_{o,xy} + z\phi_{x,y} + z\phi_{y,x} \qquad (A.8)$$

and shear strains in the rib and spar webs are given by

$$\gamma_{xz} = \phi_x \qquad (A.9)$$

$$\gamma_{yz} = \phi_y \qquad (A.10)$$

Thus, in this formulation these shear strains in the webs are constant through the depth of the wing but vary over the planform of the wing. These strains are used in the Ritz procedure, as described in Ref. 4 to produce a system of simultaneous equations which can be solved for the unknown coefficients to minimize the total energy expression. These equations have the same form as illustrated in Fig. 2. The addition of the two rotational deformation fields results in a 5 x 5 set of submatrices in the stiffness matrix.

The kinematic assumptions of first order shear deformation plate theory is used in the equivalent plate formulation of Ref. 9.

$$U = U_o + z\,\Psi_x \qquad (A.11)$$

$$V = V_o + z\,\Psi_y \qquad (A.12)$$

$$W = W_o \qquad (A.13)$$

With corresponding strains in the skins in the $x$ and $y$ directions are given by

$$\varepsilon_x = U_{o,x} + z\Psi_{x,x} \qquad (A.14)$$

$$\varepsilon_y = V_{o,y} + z\Psi_{y,y} \qquad (A.15)$$

$$\varepsilon_{xy} = U_{o,y} + V_{o,x} + z\Psi_{x,y} + z\Psi_{y,x} \qquad (A.16)$$

and shear strains in the rib and spar webs are given by

$$\gamma_{xz} = \Psi_x + W_{o,x} \qquad (A.17)$$

$$\gamma_{yz} = \Psi_y + W_{o,y} \qquad (A.18)$$

A comparison of the transverse shear rotations is given in the following sketch.

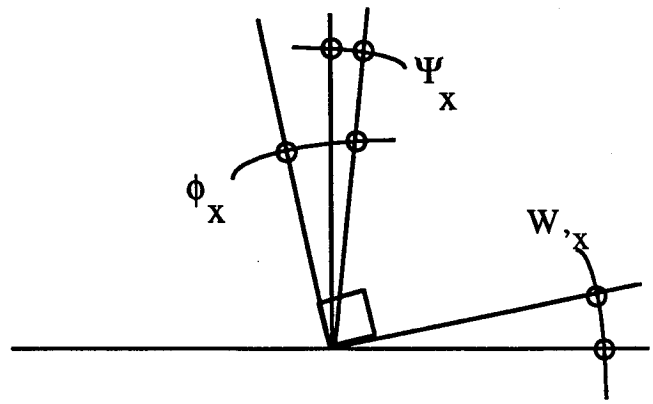


$$\phi_x = \Psi_x + W_{,x} \qquad (A.19)$$

$$\Psi_x = \phi_x - W_{,x} \qquad (A.20)$$

As shown, the formulation in this paper and the formulation in Ref. 9 are equivalent. However, the formulation in this paper offers the option to neglect the transverse shear effects in a direct manner by simply setting this rotation equal to zero through use of an input parameter to the code. The present formulation is directly suited for use in a hierarchical optimization strategy where transverse shear is neglected during early optimization cycles and is included in only the final optimization cycles where the additional accuracy is needed. In addition, for symmetric segments such as some control surfaces, $W$ only can be used with significant saving of time. The formulation in Ref. 9 does not lend itself to setting the shear terms to zero and appears to require a separate analysis code to include transverse shear considerations.

## References


1 McCullers, L. A.: Aircraft Configuration Optimization Including Optimized Flight Profiles. NASA CP-2327, Proceedings of Symposium on Recent Experiences in Multidisciplinary Analysis and Optimization, April 1984, pp. 395-412.

2 Sobieszczanski-Sobieski, J.: Multidisciplinary Design Optimization: An Emerging New Engineering Discipline. Presented at The World Congress on Optimal Design of Structural Systems, Rio de Janeiro, Brazil, August 2-6, 1993.

3 Giles, G. L.: Equivalent Plate Analysis of Aircraft Wing Box Structures with General Planform Geometry. J. of Aircraft, Vol. 23, No. 11, November 1986, pp. 859-864.

4 Giles, G. L.: Further Generalization of an Equivalent Plate Representation for Aircraft Structural Analysis. J. of Aircraft, Vol. 26, No. 1, January 1989, pp. 67-74.

[5] Giles, G. L.: Design Oriented Structural Analysis. In Advances in Structural Engineering Computing; Proceedings of 2nd International Conference on Computational Structures Technology, Athens, Greece, Aug. 30-Sept.1, 1994, pp.1-10. Also published as NASA TM-109124, June 1994.

[6] Bushnell, D. M.: Potential Impacts of Advanced Aerodynamic Technology on Air Transportation System Productivity. NASA TM 109154. September 1994.

[7] McMasters, J. H.; Kroo, I. M.; Bofah, K.; Sullivan, J. P.; Drela, M.; and Gallman, J.: Advanced Configurations for Very Large Subsonic Transport Airplanes. NASA Contract: NAS1-20269, NASA CR in preparation.

[8] Livne, E.; Sels, R. A.; and Bhatia, K. G.: Lessons from Application of Equivalent Plate Structural Modeling to an HSCT Wing. AIAA Paper No. 93-1413-CP, 34th AIAA/ASME/ASCE/AHS/ASC Structures, Structural Dynamics, and Materials Conference, La Jolla, CA, April 1993, pp. 959-969.

[9] Livne, E.: Recent Developments in Equivalent Plate Modeling for Wing Shape Optimization. AIAA Paper No. 93-1647-CP, 34th AIAA/ASME/ASCE/AHS/ASC Structures, Structural Dynamics, and Materials Conference, La Jolla, CA, April 1993, pp. 2998-3011.

[10] Igoe, W. B.: Characteristics and Status of the U.S. National Transonic Facility. Cryogenic Wind Tunnels, AGARD-LS-111, July 1980, pp. 17-1-17-11.

[11] Cavallo, P. A.: Coupling Static Aeroelastic Predictions with an Unstructured-Grid Euler/Interacting Boundary Layer Method. Master's Thesis, George Washington University Joint Institute for Advancement of Flight Sciences, NASA Langley Research Center, Hampton, VA, July 1995.

[12] Liebeck, R. H.; Page, M. A.; Rawdon, B. K.; Scott, P. W.; and Wright, R. A.: Concepts for Advanced Subsonic Transports. NASA CR-4624, September 1994.

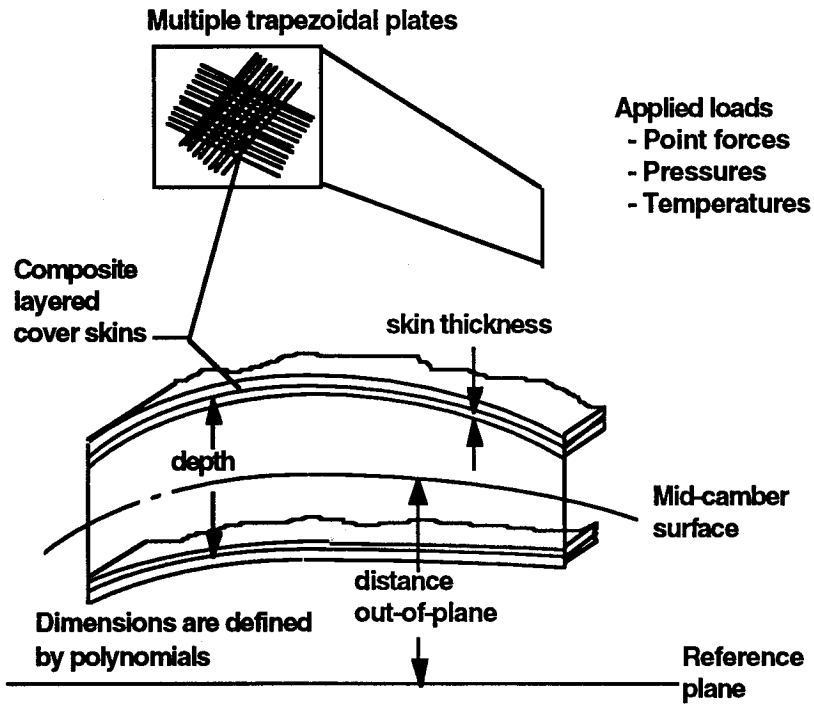


**Fig. 1 Analytical modeling of wing box structure.**

- Ritz solution technique used
- Polynomial displacement functions

$$U = \sum_i \sum_j A_{ij}\, x_i\, y_j$$
$$V = \sum_k \sum_l B_{kl}\, x^k\, y_l$$

in-plane stretching

$$W = \sum_m \sum_n C_{mn} x_m\, y^n$$

bending

- Minimization of energy

$$\Omega = 1/2 \int_{vol} (\varepsilon^T Q\, \varepsilon - 2\, \Delta T\, \alpha^T Q\, \varepsilon)\, dV$$

- Solve equations for polynomial coefficients; A, B and C

$$\begin{bmatrix} K_{uu} & K_{uv} & K_{uw} \\ K_{uv} & K_{vv} & K_{vw} \\ K_{uw} & K_{vw} & K_{ww} \end{bmatrix} \begin{Bmatrix} A_{ij} \\ B_{kl} \\ C_{mn} \end{Bmatrix} = \begin{Bmatrix} P_u \\ P_v \\ P_w \end{Bmatrix}$$

Fig. 2 Outline of equivalent plate analysis procedure.

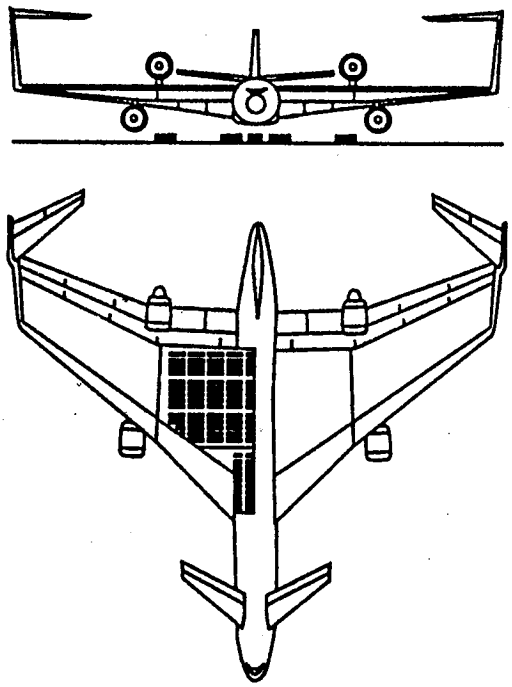

Fig. 3 C-wing aircraft configuration.

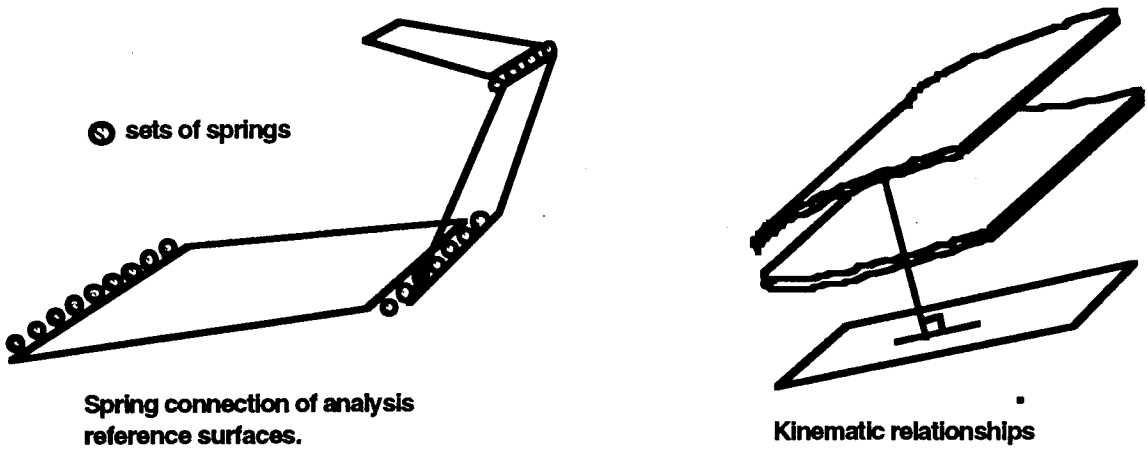


Fig. 4 Out-of-plane equivalent plate modeling.

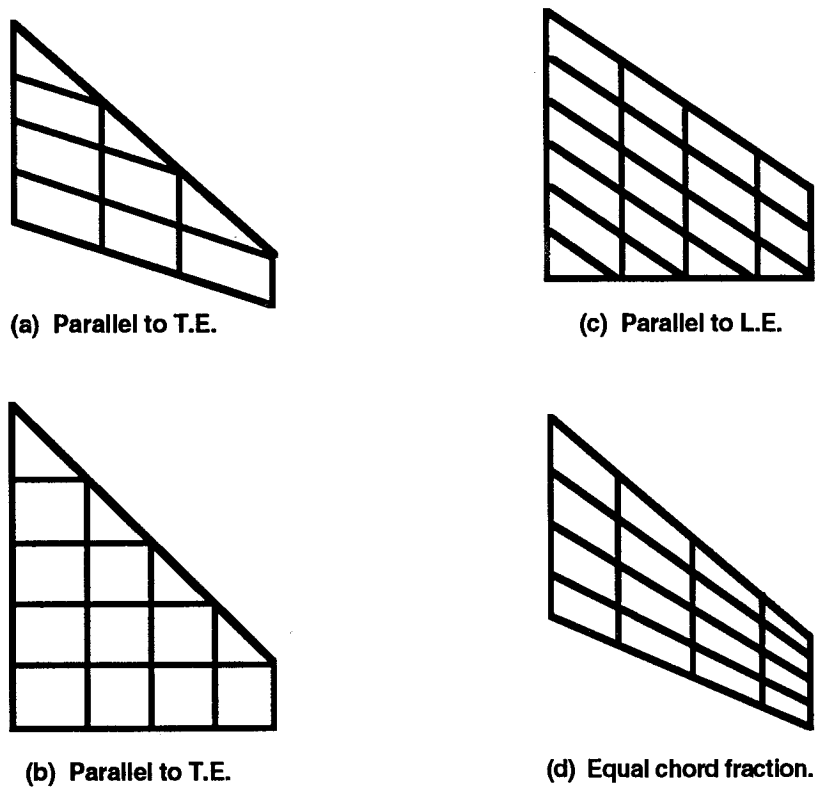


Fig. 5 Modeling of rib and spar structure.

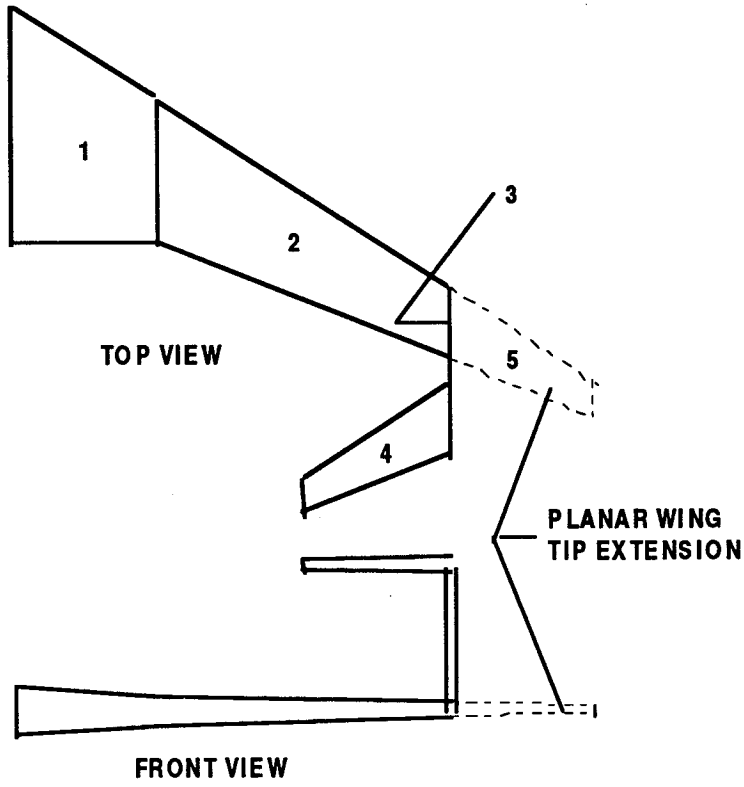


Fig. 6 C-wing and planar wing equivalent plate models.

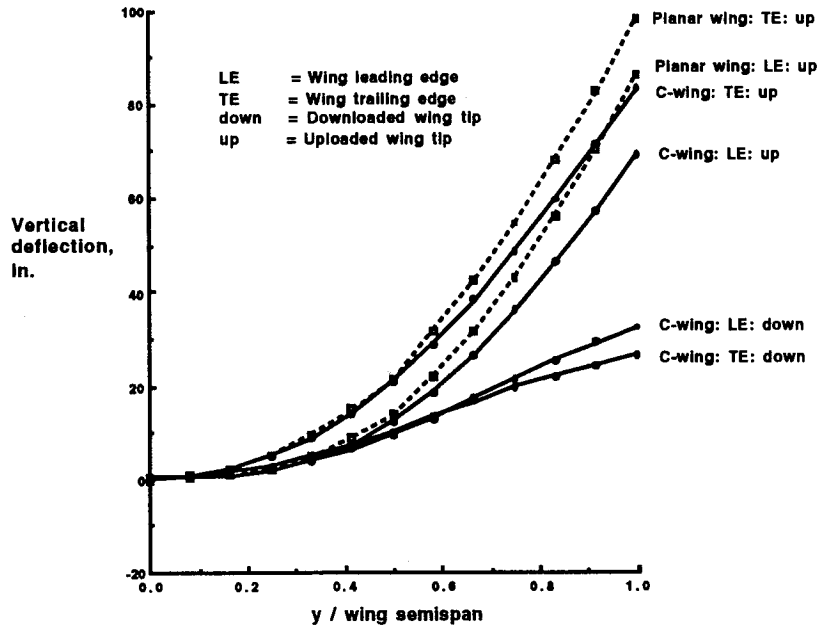


Fig. 7 Vertical deflection of wing leading and trailing edges.

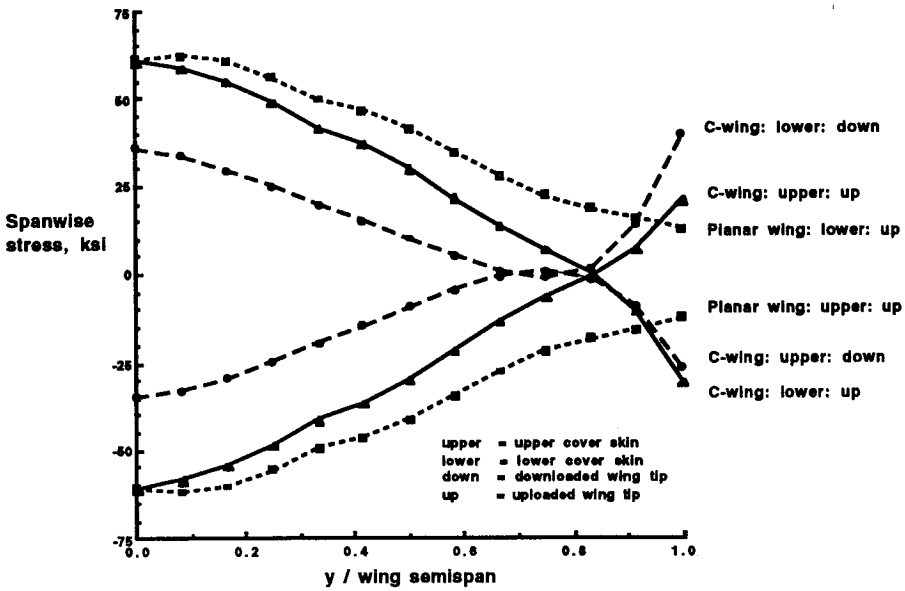


**Fig. 8 Spanwise stress in cover skin along wing trailing edge.**

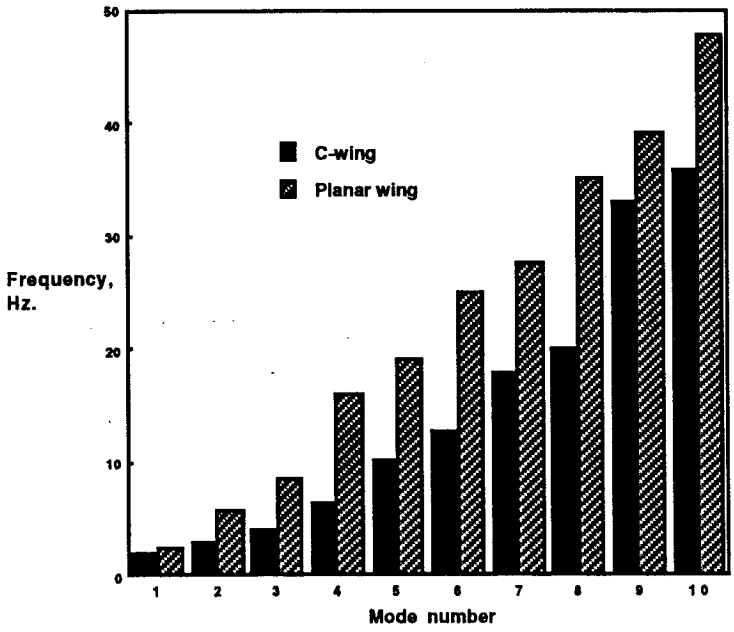


**Fig. 9 Vibration frequency comparison for C-wing and planar wing.**

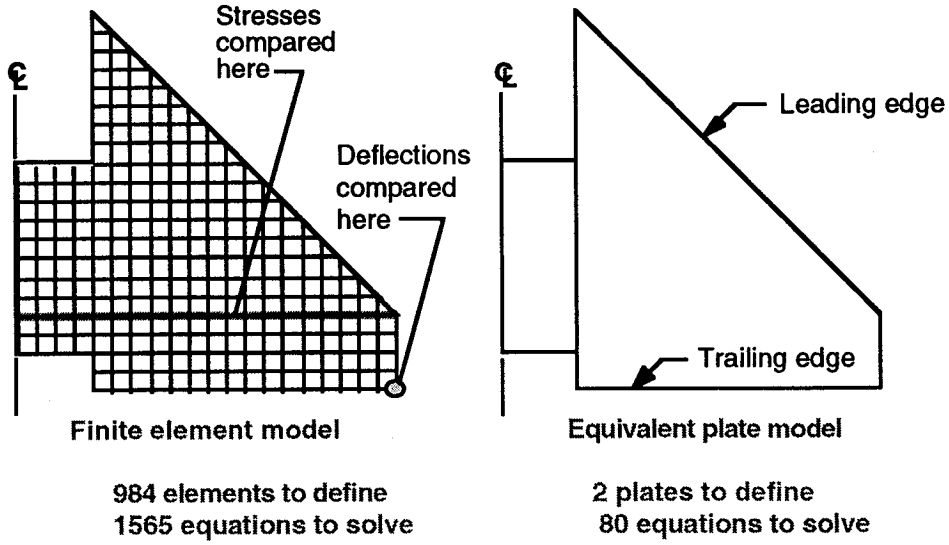


**Fig. 10 Clipped-delta wing structural models.**

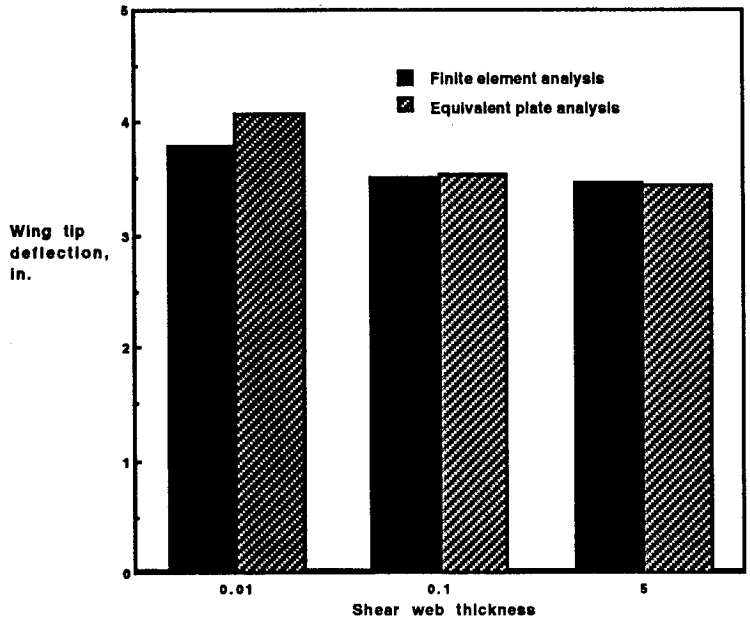


**Fig. 11 Effect of transverse shear on wing tip deflection.**

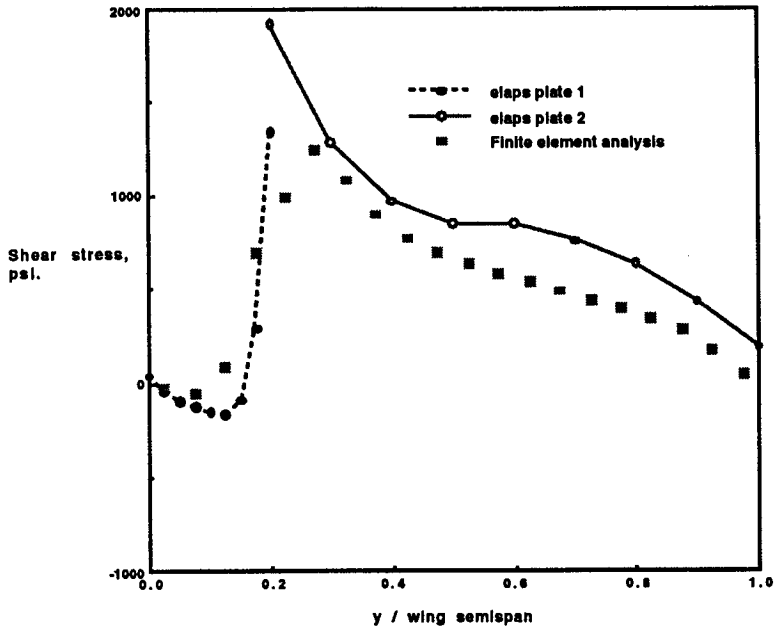


**Fig. 12 Shear stress distribution along a wing spar.**

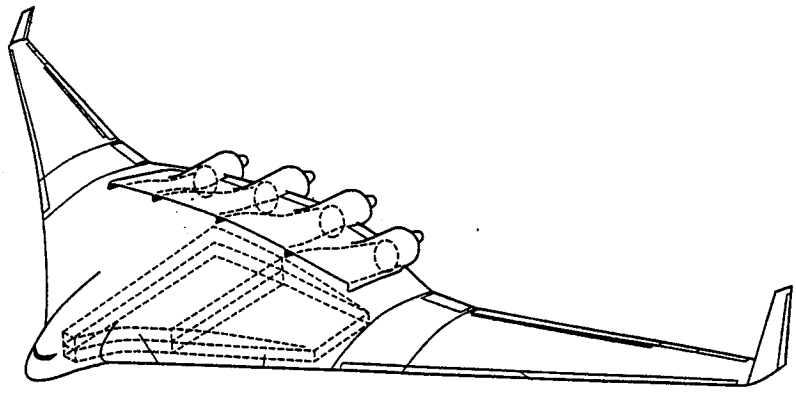

**Fig. 13 Blended-wing-body aircraft configuration.**

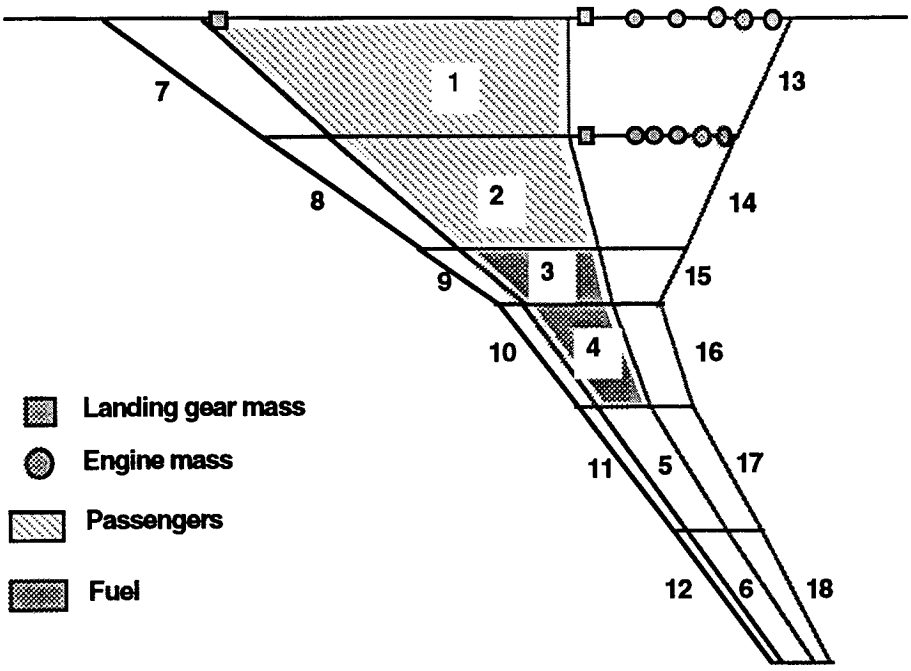


Fig. 14 Equivalent plate model of blended-wing-body.

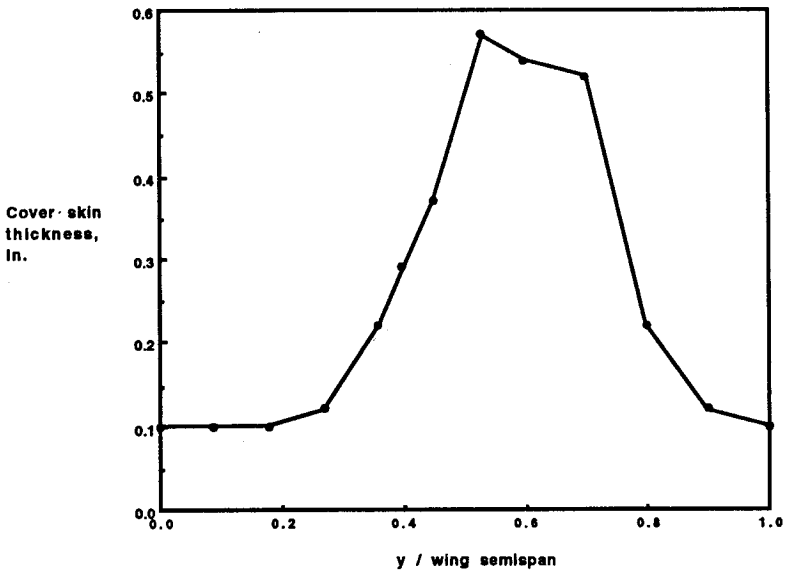


Fig. 15 Spanwise distribution of cover skin thickness.